Micromagnetic properties of MnAs(0001)/GaAs(111) epitaxial films

R. Engel-Herbert, T. Hesjedal,[a] D. M. Schaadt, L. Däweritz, and K. H. Ploog
Paul-Drude-Institut für Festkörperelektronik, Hausvogteiplatz 5-7, D-10117 Berlin, Germany

(Received 31 August 2005; accepted 15 December 2005; published online 2 February 2006)

The micromagnetic properties of MnAs thin films grown on the (111)B-oriented GaAs surface have been investigated. Compared to films grown on (001) surfaces, these films exhibit completely different domain patterns, as the *c* axis of the hexagonal unit cell is oriented normal to the surface. In the course of the first order phase transition, ferromagnetic α-MnAs forms a network of quasihexagonal areas separated by β-MnAs. We present an analysis of the micromagnetic properties based on imaging and simulations. We observe closure domains that either appear as a vortex-like state or a stripe structure. © *2006 American Institute of Physics*. [DOI: 10.1063/1.2171790]

Ferromagnet-semiconductor heterostructures are interesting candidates for novel devices combining magnetic, electronic, and optical functions.[1] Although there exist, in principle, a multitude of materials combinations, the requirement of room-temperature ferromagnetism and epitaxial film growth, i.e., high crystal quality and sharp interfaces, is seldom fulfilled. MnAs-on-GaAs is a promising material system in which spin injection has already been successfully demonstrated.[2] Epitaxial MnAs($\bar{1}$100) films grown by molecular beam epitaxy on GaAs(001) exhibit a coupled magnetostructural first order phase transition from the ferromagnetic, hexagonal α-phase to the paramagnetic, orthorhombic β-phase at a temperature of about 40 °C.[3–5] During the phase transition, the lattice spacing within the hexagonal plane (*a* axes) is discontinuous, while the lattice spacing along the *c* axis remains continuous.[6] In epitaxial films on GaAs(001) with the *c* axis in-plane and the prismatic ($\bar{1}$100) plane the growth plane,[5] the constraints on MnAs imposed by the substrate alter the magnetic and structural behavior significantly, leading to the formation of a periodic α-β-stripe structure.[7]

In contrast, the epitaxial growth of MnAs on the GaAs(111)B surface results in the *c* axis being perpendicular to the growth plane, i.e., the growth plane is the basal plane of the hexagonal unit cell (see Fig. 1).[8,9] The presence of a second orientation where the growth plane is the MnAs($\bar{1}$101) lattice plane is avoided by choosing the appropriate growth conditions.[10] As a result of the first-order nature of the magnetostructural phase transition, the ferromagnetic long-range order is observable for temperatures above the phase transition temperature of bulk MnAs crystals of 40 °C.[11–13] The phase transition proceeds over a large temperature range resulting in a coexistence of α- and β-MnAs.[11] Etching experiments revealed that α-MnAs forms partially connected hexagonal islands, surrounded by β-MnAs.[14] So far, tunneling magnetoresistance in MnAs(0001)–AlAs(111)–MnAs(0001) trilayer heterostructures has been demonstrated[15] and the electronic and magnetoresistive properties have been investigated.[16,17] Detailed investigations of the growth morphology have been performed employing scanning tunneling microscopy and reflection high-energy electron diffraction in order to find the optimal growth conditions for smooth MnAs(0001) surfaces.[10,18–20] The magnetization curves are rounded[12] and nearly isotropic in the hexagonal plane (i.e., measured along the [11$\bar{2}$0] and [$\bar{1}$100] directions).[21] Up to now, no correlation between the topographic structure and the magnetic properties have been found.[22] In this letter, we present a study of the micromagnetic properties of MnAs(0001) films on GaAs(111)B and explain the observed domain structures with the help of micromagnetic simulations.

MnAs films were grown by molecular beam epitaxy on commercially available epiready GaAs(111)B substrates at a temperature of 250 °C.[10] The sample was capped with a ≈300-nm-thick As layer. After the transfer in an inert gas atmosphere to the "Nanospectroscopy" beamline at Elettra (Trieste, Italy), the sample was decapped at ≈325 °C. Combined low energy electron microscopy (LEEM) and x-ray magnetic circular dichroism photoemission electron microscopy (XMCDPEEM) was performed at various temperatures in the α-β-phase coexistence regime, revealing the topography and the local magnetization, respectively.[12]

XMCDPEEM imaging of the local magnetization **M** uses the secondary electrons created in the photoionization process of the Mn L_3 edge. The secondary electron yield depends on the helicity $\boldsymbol{\sigma}$ of the incident, circularly polarized light and is proportional to $\boldsymbol{\sigma}\cdot\mathbf{M}$. In order to obtain the helicity-dependent magnetic contrast, images recorded with opposite helicity are subtracted. The magnetic contrast reveals the direction, and to a certain degree also the magni-

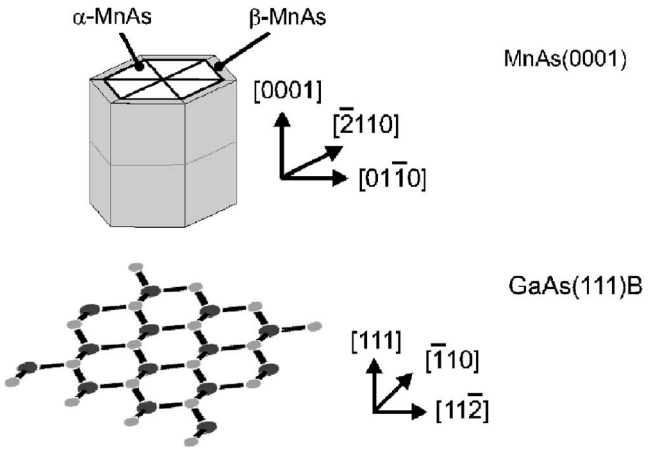

FIG. 1. Epitaxial orientation of MnAs(0001) on GaAs(111)B. The hexagonal α-MnAs and orthorhombic β-MnAs unit cells are shown on top.

[a]Electronic mail: hesjedal@pdi-berlin.de

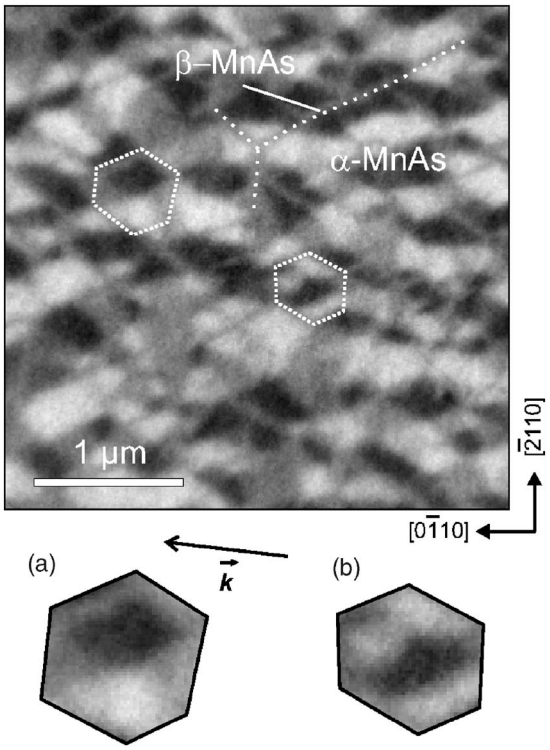

FIG. 2. Micromagnetic XMCDPEEM image of a 270-nm-thick MnAs film on GaAs(111)B recorded at 19 °C. The wave vector **k** of the incident light is indicated below. Ferromagnetic α-MnAs arranges in a network of quasihexagonal structures, separated by nonmagnetic β-MnAs. Two closeups of quasihexagonal elements reveal the common magnetization patterns: (a) vortex-like domain and (b) distorted stripe domain.

tude, of the local magnetization $\mathbf{M}(\mathbf{r})$.[23] The plane of incidence of the light was slightly misaligned with a MnAs[$\bar{2}$110] axis. The magnetic contrast reaches from dark to bright, corresponding to the magnetization ranging from fully parallel to fully antiparallel, respectively. Neutral grey contrast is obtained for nonmagnetic areas, as well as for a vanishing projection of the magnetization vector along the selected MnAs[$\bar{2}$110] axis ($\mathbf{M} \perp \boldsymbol{\sigma}$).

The micromagnetic domain pattern obtained by XMCD-PEEM imaging (Fig. 2) shows all contrast levels reaching from bright ($\mathbf{M}\uparrow\uparrow\mathbf{k}$) to dark ($\mathbf{M}\uparrow\downarrow\mathbf{k}$) in the ferromagnetic areas, depending on the projection of the magnetization **M** onto the wave vector **k** of the incident light. The coexisting nonmagnetic β-MnAs areas exhibit a neutral grey contrast and form a honeycomb-like network that is indicated by a dotted line. The exact position of the β-MnAs can be obtained from LEEM imaging[24] at the sample sample spot and is also confirmed by etching experiments.[14] Two representative quasihexagonal α-MnAs areas are highlighted and zoomed into in (a) and (b). The first structure shown in (a) exhibits three contrast levels, where the dark and bright contrast areas occupy each two of the hexagonal segments, while a similar, neutral grey level is seen in the remaining two segments. This contrast belongs to a vortex-like state, as will be shown in Fig. 3(a). The second domain pattern depicted in Fig. 2(b) shows basically three areas with largely opposite magnetization. The three stripe-like domains further exhibit a fine structure.

In principle, the magnetic easy plane character of the MnAs(0001) surface leads to a number of domain configurations as no direction is preferred, which can be held responsible for the difficulties in interpreting the magnetic force microscopy observations.[22] Moreover, MnAs-on-GaAs(111) behaves like a nanopatterned system, as the ferromagnetic material forms a network of quasihexagonal structures that can be in fact seen as hexagonal columns, surrounded by nonmagnetic material (see Fig. 1).[14] Furthermore, the β-MnAs surrounding the columns is known to be highly strained,[25] which may lead to an additional magnetic anisotropy. To understand the micromagnetic contrast of MnAs on GaAs(111) and its origin, we performed two-dimensional micromagnetic simulations. We assumed an array of hexagonal, ferromagnetic α-MnAs columns with a side length of 300 nm, separated by 50 nm wide nonmagnetic material. Thus, the lateral size of the simulated structure is the same as the average size of the observed quasihexagonal structures. The simulated hexagonal pattern

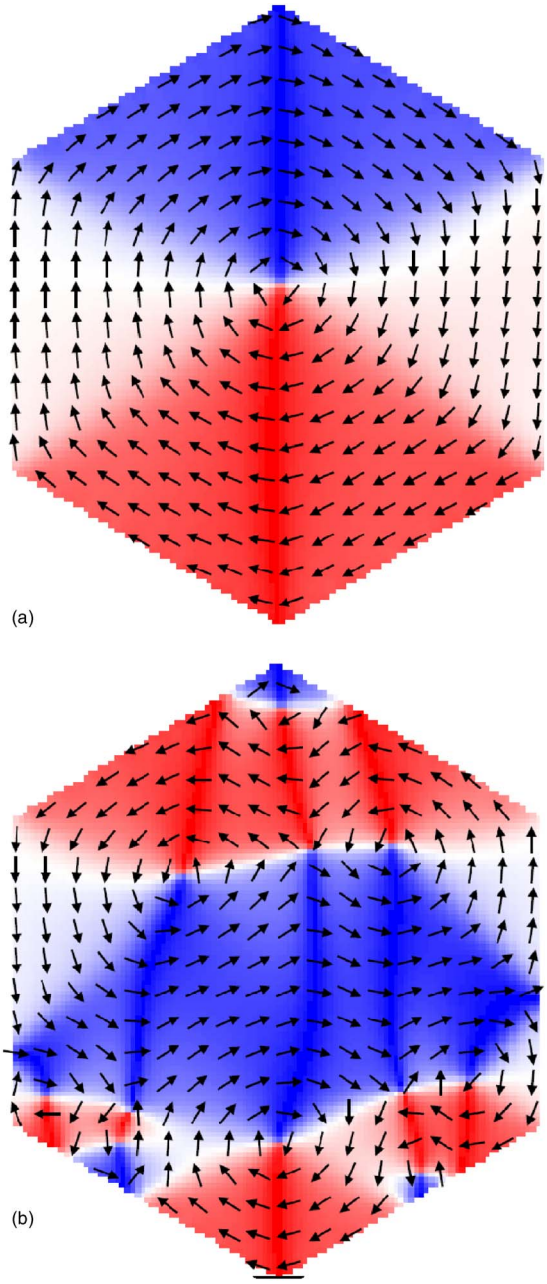

FIG. 3. (Color online) Calculated magnetization vector field in the remanent state of two representative domain patterns: (a) vortex-like domain pattern and (b) (distorted) stripe domain pattern.

measured $1585 \times 1640\ \mathrm{nm}^2$. The two-dimensional unit cell of the simulation was chosen to be $(5\ \mathrm{nm})^2$ which has the same dimensions as the magnetocrystalline and the magnetostatic exchange lengths in MnAs. We have chosen reasonable parameters for the two-dimensional simulations as follows: exchange stiffness constant $A = 1.0 \times 10^{-11}\ \mathrm{J/m}$,[26] saturation magnetization $M_s = 8 \times 10^5\ \mathrm{A/m}$ (from magnetization curve measurements), and an uniaxial magnetocrystalline anisotropy with the constants $K_{u1} = -7.2 \times 10^5\ \mathrm{J/m}^3$ and $K_{u2} = -3.6 \times 10^5\ \mathrm{J/m}^3$.[27] The axis of the magnetocrystalline anisotropy (c axis) is collinear with the z axis of the coordinate system. The thickness of the simulated film was set to 50 nm, as we do not expect a thickness dependence of the magnetization distribution.

A solution of the energy minimum is sought by integrating the Landau-Lifshitz-Gilbert equation. We used a simple Euler integration with variable time-step size, the stability is assured by monitoring the total energy of the system. As an initial configuration, the ferromagnetic hexagons were assumed to be randomly magnetized. The random magnetization was allowed to relax in zero applied field and the result is shown in Fig. 3 for the two common states—the vortex-like state (a) and the (distorted) stripe state (b). In the vortex-like state, the magnetization is largely parallel to the respective hexagonal boundary, leading to a domain pattern with a sixfold symmetry. The arrows represent the direction of the local magnetization $\mathbf{M}(\mathbf{r})$. In the stripe state, basically three predominant magnetization directions can be seen, leading to the observed stripe-like contrast. A closer look at the domain structure reveals a number of neighboring vortex-like states. The stripe state is also governed by coupling across the β-MnAs spacers. Because the magnetocrystalline anisotropy as well as the shape anisotropy impede an out-of-plane magnetization, it is the demagnetization and exchange energies that govern the formation of domains. Thus, MnAs(0001) on GaAs(111)B behaves in this respect like a soft magnetic material.

The simulation of the hexagonal structure in Cartesian coordinates leads to structural boundaries that are approximated by a staircase along the grid lines. The approximated magnetic boundary conditions can cause deviations to the stray field.[28] Nevertheless, already the initial magnetic configuration shows that the magnetization vector is parallel to the boundary of the hexagon. Thus, the staircase approximation seems applicable for the present magnetic problem.

In conclusion, we have presented micromagnetic imaging of MnAs(0001) films on GaAs(111)B surfaces. The coexisting ferromagnetic α- and nonmagnetic β-phase form a network of connected quasihexagonal α-MnAs separated by β-MnAs. The magnetic easy plane character of the film leads to a complex magnetic domain pattern. Two common domain states—a vortex-like state and a striped state—were identified in the micromagnetic imaging and confirmed by the simulations.

The authors would like to thank J. Herfort for helpful discussions and Dr. E. Bauer and his co-workers for the XMCDPEEM image. Part of this work was sponsored by the BMBF of Germany.

[1] G. A. Prinz, Science **250**, 1092 (1990).
[2] M. Ramsteiner, H. Y. Hao, A. Kawaharazuka, H. J. Zhu, M. Käastner, R. Hey, L. Däweritz, H. T. Grahn, and K. H. Ploog, Phys. Rev. B **66**, 081304(R) (2002).
[3] M. Tanaka, J. P. Harbison, M. C. Park, Y. S. Park, T. Shin, and G. M. Rothberg, J. Appl. Phys. **76**, 6278 (1994).
[4] M. Tanaka, Physica E (Amsterdam) **2**, 372 (1998).
[5] F. Schippan, G. Behme, L. Däweritz, K. H. Ploog, B. Dennis, K.-U. Neumann, and K. R. A. Ziebeck, J. Appl. Phys. **88**, 2766 (2000).
[6] B. T. M. Willis and H. P. Rooksby, Proc. Phys. Soc. London, Sect. B **67**, 290 (1954).
[7] T. Plake, M. Ramsteiner, V. M. Kaganer, B. Jenichen, M. Kästner, L. Däweritz, and K. H. Ploog, Appl. Phys. Lett. **80**, 2523 (2002).
[8] Y. Morishita, K. Iida, J. Abe, and K. Sato, Jpn. J. Appl. Phys., Part 2 **36**, L1100 (1997).
[9] V. H. Etgens, M. Eddrief, D. Demaille, Y. L. Zheng, and A. Ouerghi, J. Cryst. Growth **240**, 64 (2002).
[10] M. Kästner, L. Däweritz, and K. H. Ploog, Surf. Sci. **511**, 323 (2002).
[11] B. Jenichen, V. M. Kaganer, M. Kästner, C. Herrmann, L. Däweritz, K. H. Ploog, N. Darowski, and I. Zizak, Phys. Rev. B **68**, 132301 (2003).
[12] L. Däweritz, C. Herrmann, J. Mohanty, T. Hesjedal, K. H. Ploog, E. Bauer, A. Locatelli, S. Cherifi, R. Belkhou, A. Pavlovska, and S. Heun, J. Vac. Sci. Technol. B **23**, 1759 (2005).
[13] A. Ney, T. Hesjedal, L. Däweritz, R. Koch, and K. H. Ploog, J. Magn. Magn. Mater. **288**, 173 (2005).
[14] Y. Takagaki, E. Wiebicke, L. Däweritz, and K. H. Ploog, Appl. Phys. Lett. **85**, 1505 (2004).
[15] S. Sugahara and M. Tanaka, Appl. Phys. Lett. **80**, 1969 (2002).
[16] K. Narita and M. Shirai, Physica E (Amsterdam) **10**, 433 (2001).
[17] K. J. Friedland, M. Kästner, and L. Däweritz, Phys. Rev. B **67**, 113301 (2003).
[18] J. Sadowski, J. Kanski, L. Ilver, and J. Johansson, Appl. Surf. Sci. **166**, 247 (2000).
[19] S. Sugahara and M. Tanaka, J. Appl. Phys. **89**, 6677 (2001).
[20] A. Ouerghi, M. Marangolo, M. Eddrief, S. Guyard, V. H. Etgens, and Y. Garreau, Phys. Rev. B **68**,115309 (2003).
[21] M. Kästner, L. Däweritz, and K. H. Ploog (unpublished).
[22] M. Mizugushi, H. Kuramochi, J. Okabayashi, T. Manago, and H. Akinaga, Mater. Trans., JIM **44**, 2578 (2003).
[23] E. Bauer, A. Pavlovska, S. Cherifi, S. Heun, A. Locatelli, R. Belkhou, J. A. C. Bland, M. Kläui, C. A. F. Vaz, L. J. Heyderman, J. Shi, and W. C. Uhlig, ELETTRA highlights **42** (2002–2003).
[24] E. Bauer, A. Pavlovska, R. Belkhou, S. Cherifi, S. Heun, and A. Locatelli (unpublished).
[25] N. Mattoso, M. Eddrief, J. Varalda, A. Ouerghi, D. Demaille, V. H. Etgens, and Y. Garreau, Phys. Rev. B **70**, 115324 (2004).
[26] R. Engel-Herbert, T. Hesjedal, and D. M. Schaadt (submitted).
[27] J. Lindner, T. Tolinski, K. Lenz, E. Kosubek, H. Wende, K. Baberschke, A. Ney, T. Hesjedal, C. Pampuch, R. Koch, L. Däweritz, and K. H. Ploog, J. Magn. Magn. Mater. **277**, 159 (2004).
[28] C. J. Garcia-Cervera, Z. Gimbutas, and E. Weinan, J. Comput. Phys. **184**, 37 (2003).